

RSC Advances



This is an *Accepted Manuscript*, which has been through the Royal Society of Chemistry peer review process and has been accepted for publication.

Accepted Manuscripts are published online shortly after acceptance, before technical editing, formatting and proof reading. Using this free service, authors can make their results available to the community, in citable form, before we publish the edited article. This *Accepted Manuscript* will be replaced by the edited, formatted and paginated article as soon as this is available.

You can find more information about *Accepted Manuscripts* in the [Information for Authors](#).

Please note that technical editing may introduce minor changes to the text and/or graphics, which may alter content. The journal's standard [Terms & Conditions](#) and the [Ethical guidelines](#) still apply. In no event shall the Royal Society of Chemistry be held responsible for any errors or omissions in this *Accepted Manuscript* or any consequences arising from the use of any information it contains.

1 Through-holes, cavities and perforations in 2 polydimethylsiloxane (PDMS) chips

3
4 Tomas Silva Santisteban^{1,2}, Roland Zengerle^{2,3}, Matthias Meier^{1,2,*}

5
6
7 ¹Microfluidic and Biological Engineering, IMTEK - Department of Microsystems Engineering,
8 University of Freiburg, Georges-Koehler-Allee 103, 79110 Freiburg, GERMANY

9 ²BIOSS - Centre for Biological Signalling Studies, University of Freiburg, GERMANY

10 ³Laboratory for MEMS Applications, IMTEK - Department of Microsystems Engineering,
11 University of Freiburg, GERMANY
12

13 *Correspondence should be addressed to: matthias.meier@imtek.de
14

15 Abstract

16 We present a method to fabricate through-holes between 10 to 180 μm between
17 polydimethylsiloxane (PDMS) layers of microfluidic large-scale integration platforms.
18 Therefore we employed standard PDMS spin-coating processes onto silicon molds
19 with microstructures formed from SU-8 and AZ photoresists. Our approach is based
20 on the modification of the surface polarity of the PDMS prototyping molds by a 250
21 nm thick layer of octafluorocyclobutane (C_4F_8), which resulted in a contact angle of
22 125 ± 3 degrees for water. This super hydrophobic surface repelled PDMS from
23 microstructures protruding out of the spin coated PDMS layer. Subsequently, we
24 applied and characterized the C_4F_8 coating for the robust fabrication of interlayer
25 connectors between PDMS membranes of 40 μm thickness. To enable embedding of
26 through-holes, perforations and/or cavities in very thin layers of PDMS (<20 μm) we
27 mixed PDMS with a PDMS based silicone oil to reduce its viscosity. In difference to
28 previous attempts to lower the viscosity of PDMS using organic solvents, the silicone
29 oil cross-linked to PDMS and was thus, unable to freely diffuse into the polymerized
30 PDMS. This reduces the risk for bleeding of hazardous components in biological
31 applications. Finally, we manufactured a three layer mLSI chip with integrated cavities
32 for catching fluorescently labeled beads and cells. The presented process parameters
33 can easily be adapted to specific needs in fabrication of multi-layer PDMS
34 arrangements by following the systematic parameter screening.
35
36
37
38
39

1

2 **Introduction**

3 Microfluidic large-scale integration (mLSI) is regarded as an enabling technology for
4 systems biology research. Since the invention of the pneumatic membrane valves on
5 polydimethylsiloxane (PDMS) chip platforms, many different design elements
6 including pumps, oscillators, or shift registers have been developed.¹⁻³ The mLSI
7 design elements were generated with standard photolithography and rapid
8 prototyping workflows, with minimal instrumentation requirements.⁴ An early research
9 goal for mLSI technologies was to maximize the integration density of design
10 elements. Although this density continuously increased, a natural limit is set by the
11 dimensions of the object of study, e.g. the size of a biological cell.⁵ Therefore, current
12 research is focused on the development of multilayer arrangements, which enable to
13 implement more functions within the same footprint, while still retaining the existing
14 size of the design elements. However, the latter requirement is not specified
15 anymore.⁶

16 A central element to increase the density of fluid operations on PDMS chips is the
17 interlayer connector named 'via'.⁷ This through-hole enables the bridging of two flow
18 streams at fluid cross-junctions with a minimal increase in the overall chip area. Initial
19 manufacturing procedures of vias were based on a simple photolithography process,
20 in which pillars on rapid prototyping molds with heights ranging from 20 to 50 μm
21 were used. Upon spinning a PDMS membrane with a thickness lower than that of the
22 pillar structures onto the mold, the pillars protrude out of the PDMS and leave a
23 through-hole after layer bonding and demolding. Despite the simplicity of the process,
24 the vias did not find entry on mLSI chip platforms as the manufacturing process is
25 unstable. Often vias remained closed owing to the residual PDMS membranes
26 present on top of the pillars after spin coating. Alternative manufacturing processes
27 for vias e.g. laser drilling⁸, electrochemical micromachining⁹, clamping gaskets¹⁰, dry
28 etching¹¹, photolithographic surface micromachining¹², or the spatial inhibition of the
29 PDMS curing over the via areas¹³ added a lot of complexity to the manufacturing
30 process.

31 The production of perforated PDMS membranes (PMs) also presents us with
32 similar problems. In fact, PMs can be regarded as arrays of via elements at short
33 pitch distances. PMs are attractive design elements to separate and trap particles or
34 biological cells in small cavities on mLSI chips.¹⁴⁻¹⁶ The manufacturing protocols for
35 PMs are similar to those for via elements, with the exception that most applications
36 demand PDMS membranes that are $<20 \mu\text{m}$ thick. Thinner PDMS membranes are
37 obtained by mixing PDMS with organic solvents to decrease its viscosity during the

1 spin coating process.^{17,18} However, after the curing process, the residual organic
 2 solvents in the PDMS make the prototyping method incompatible for biological cell
 3 culture devices. Therefore, a simple manufacturing process for generating through-
 4 holes within the PDMS layers could leverage the application of vias and perforated
 5 membranes.

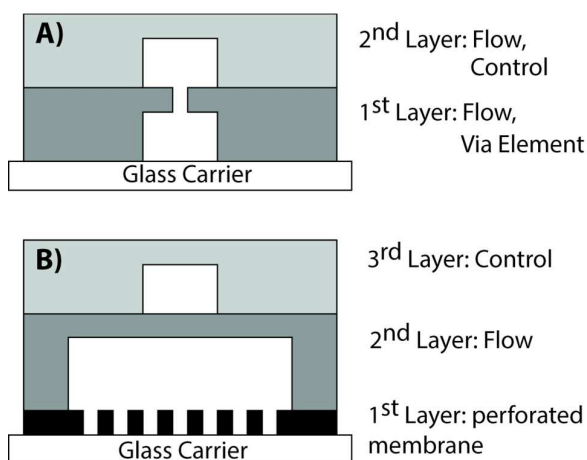
6 Here, we present a two-step manufacturing procedure for the production of reliable
 7 vias and perforated PDMS membranes with thicknesses ranging from 10 to 40 μm for
 8 microfluidic large-scale integration technologies. In the first step, we altered the
 9 surface properties of standard silicon molds with octafluorocyclobutane (C_4F_8) for
 10 rapid PDMS prototyping and systematically determined the range of process
 11 parameters enabling reliable implementation of via elements. In the second step, we
 12 reduced the PDMS viscosity with biologically compatible silicone oil to obtain thin
 13 perforated membranes. These simplified protocols can be combined to build robustly
 14 complex fluid routing operations or biological cell sorting systems, and trapping
 15 elements in multi-layered PDMS chips.

16

17 **Experimental design**

18 Within this work we designed and fabricated two PDMS chips, i.e. one with via
 19 elements and another with a perforated membrane, which required two or three
 20 PDMS layers, respectively. The cross sections and PDMS layer arrangement of both
 21 chips are depicted in Figure 1.

22



23

24

25 Figure 1. PDMS layer arrangement for via and perforated membrane fabrication. A)
 26 The via element is included as through-hole within the lower PDMS layer. B) The
 27 perforated membrane is included within the mLSI chip as bottom layer and acts as an
 28 array of microcavities. The here presented production process can alternatively be

1 applied for including the perforated membrane between the fluid flow and pneumatic
2 control layer.

3 4 *Design and fabrication of the PDMS molds*

5 Chip layouts were drawn in AutoCAD and ordered as emulsion masks
6 (bvm.maskshop, Obertshausen, Germany) with a resolution of 50.000 dpi. For each
7 PDMS layer a silicon mold was fabricated. Chip with vias: Microstructures on the
8 mold for the 1st PDMS layer were 120 x 20 μm (width x height) and fabricated with the
9 photoresist AZ-40XT (MicroChemicals, Germany). To obtain a semi-round channel
10 profile, the AZ photoresist were reflowed for 4h at 200°C on a hot plate. On top of the
11 AZ layer, SU-8 (microchem, MI, USA) microstructures with the shapes of round pillars
12 were deposited in order to implement via elements. The pillar sizes changed between
13 chips (see below). Microstructures on the silicon mold for the 2nd PDMS layer were
14 fabricated with SU-8 and had a width and height of 120 and 40 μm , respectively. Chip
15 with perforated membrane: Microstructures on the mold for 1st PDMS layer forming
16 the perforated membrane were fabricated by SU-8, and had a width and height of 180
17 μm and 40 μm , respectively. Microstructures on mold for the 2nd and 3rd PDMS,
18 resembled the manufacturing processes for production of the molds for the 1st and 2nd
19 PDMS layer of the chip with via elements expect that the SU-8 layer for the vias
20 elements were omitted.

21 22 *Coating of the PDMS molds*

23 All molds were coated with a 250 nm octafluorocyclobutane (C_4F_8) layer that was
24 deposited by an ion induced plasma (ICP) process. The parameters for the deposition
25 process within the ICP machine (Surface Technology Systems, Newport, UK) were
26 600 W for the RF coil, a manual pressure of 65% in the deposition chamber, and a
27 deposition rate of 85 standard cubic centimeter per minute (sccm) for the C_4F_8 .
28 Alternatively, it is possible to deposit C_4F_8 within a regular plasma oxidation chamber.

29 30 *Prototyping of the PMDS chip with via elements*

31 Via elements were included within a chip with two PDMS layers, where layers were
32 bonded together with the off-ratio method.¹⁹ Briefly, the upper and lower PDMS layer
33 had a 5:1 and 20:1 ratio of the Sylgard 184 (Dow Corning, Midland, MI) base material
34 to the cross-linker, respectively. The optimal spin parameters for the lower via layer
35 were determined as given below. Both the layers were half-cured for 15–18 minutes
36 at 80°C. After the alignment of the layers, the chip was heated for another 60 minutes
37 at 80°C before it was plasma bonded to the glass carrier.

1

2 *Prototyping of PDMS chips with perforated membranes*

3 The PDMS chips with PMs comprised three layers. The PM was incorporated as the
4 bottom layer. The PMs were fabricated with Sylgard 184 (10:1) mixed with different
5 ratios of the silicone oil Element14 PDMS 50-E (Momentive, USA), a low viscosity
6 PDMS-based oil. The top two PDMS layers were fabricated and bonded to each other
7 using a procedure similar to that for the via chips. The PM was bonded to the upper
8 two layers by plasma activation.

9

10 **Results and Discussion**11 *Via structure elements*

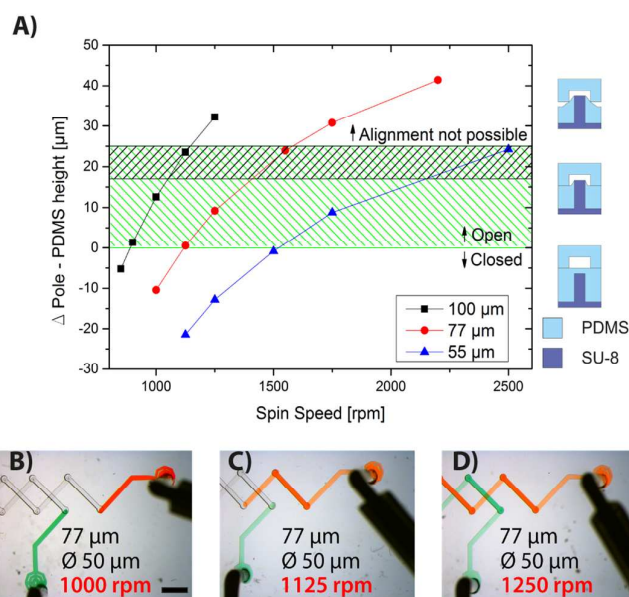
12 Standard mold fabrication protocols for PDMS end with a silanization step.²⁰ Silane
13 acts as a lubricant layer and improves the release of PDMS by reducing the surface
14 energy of the silicon wafer and the patterned photoresist features on it. While this
15 method is sufficient for robustly demolding the PDMS, it is not sufficient for avoiding
16 the residual PDMS on top of SU-8 via elements during a spin coating process,
17 especially at small margins. Therefore, we replaced the silane coating with a C₄F₈
18 coating. It has been reported that the SU-8 surfaces and the silane coated SU-8 have
19 water contact angles between 75 and 100 degrees. For a silicon mold coated with
20 250 nm C₄F₈ layer, we determined the water surface contact angle to be 125 ± 3
21 degrees. In order to investigate if this change in the surface energy changed the
22 wettability of the PDMS on the SU-8 poles for via construction, we fabricated two-
23 layered microfluidic chips with a simple 2-dimensional crossing channel network (see
24 figure 2B). During the fabrication process, we systematically determined the mutual
25 dependence between the spin rates for the coating molds with uncured PDMS and
26 the protrusion height of the poles on the mold for the production of functional via
27 elements. In particular, three molds for the lower PDMS layer were manufactured with
28 pole heights of 55, 77, and 100 μm, respectively.

29 The result is shown in figure 2A, where we have plotted the length of the SU-8 pole
30 that protrudes from the PDMS layer, i.e., the difference between the height of the SU-
31 8 pole and the thickness of the PDMS layer, versus the spin speed used to coat
32 molds with uncured PDMS. The absolute height of the PDMS layer was between 25
33 and 125 μm at 750 and 2500 rpm, respectively, and was calculated from the spin-
34 coating speed, by considering reference values.²¹ Clearly, when the height difference
35 between the poles and the PDMS is < 0 μm, the SU-8 poles are completely covered
36 by the PDMS, and the vias remain closed. Upon slightly decreasing the height of the

1 PDMS layer relative to the pole height, the vias remained open. When the height
 2 difference between the poles and PDMS layer is more than 25 μm , the top and lower
 3 PDMS layers get misaligned owing to the steric hindrance of the poles as illustrated in
 4 the pictograms of figure 2A. Although we countered the poles on the flow layer with
 5 complementary holes (diameter: 250 μm ; depth: 40 μm) in the upper PDMS layer, the
 6 bonding of the two PDMS layers was hindered. The green dashed area shows the
 7 parameter region for the functional robust fabrication of vias onto the C_4F_8 coated
 8 molds.

9 For comparison, we screened the same parameter space for the production of vias
 10 on the silanated PDMS molds. The green/black shaped area in figure 2A indicates the
 11 region from where the functional vias were obtained. This result makes an argument
 12 that a change in the surface property causes the repulsion of the PDMS from the pole
 13 tops. A change of the C_4F_8 layer thickness from 100 to 500 nm was neither changing
 14 the water contact angle on the surface nor did affect the PDMS de-molding process.
 15 In conclusion, the C_4F_8 coating on the PDMS prototyping molds increases the
 16 parameter region for the production of vias. This study offers a method for the
 17 fabrication of through-holes in the thinner PDMS layers.

18



19

20 Figure 2. Mutual dependence of the PDMS layer thickness and the protrusion pole
 21 height for the fabrication of vias within the two-layered PDMS chips. A) The plot
 22 shows the protrusion heights of the poles (55, 77, and 100 μm) from the PDMS layers
 23 spin coated for 30 seconds at various spin speeds. The resulting height of the PDMS
 24 layer formed by the 20:1 ratios was calculated from the reference values, whereas the

1 pole heights were experimentally measured. The green and green/black dashed
2 areas denote the parameter space for the open via elements on the C_4F_8 and silane
3 coated molds. The pictograms on the right side of the figure illustrate the different
4 layer alignment regimes. B-D) Images of the two-layered PDMS chips with 2D
5 crossing flow channels enabled by via elements. The via elements are closed, not
6 robustly open, and open within the figures B, C, and D, respectively. The flow
7 channels are filled with green and red colored aqueous solutions. The scale bar in
8 figure B corresponds to 1mm.

9 10 *Perforated PDMS membranes*

11 PDMS membranes with film thicknesses $\leq 20 \mu\text{m}$ have been fabricated by lowering
12 the viscosity of the PDMS base material with organic solvents during the spin-coating
13 process. The prototyping of thin perforated membranes failed either owing to the
14 rupture of the membrane during demolding or because of the incomplete removal of
15 PDMS from the pole structures. It has been previously shown²² that the wettability of
16 the molds with dense feature structures (unlike the wettability of the via elements)
17 changes with respect to the aspect ratio, area, and pitch distance of the features.
18 Therefore, we tested if the C_4F_8 coating of molds with an array of SU-8 poles can be
19 used for the fabrication of perforated PDMS membranes.

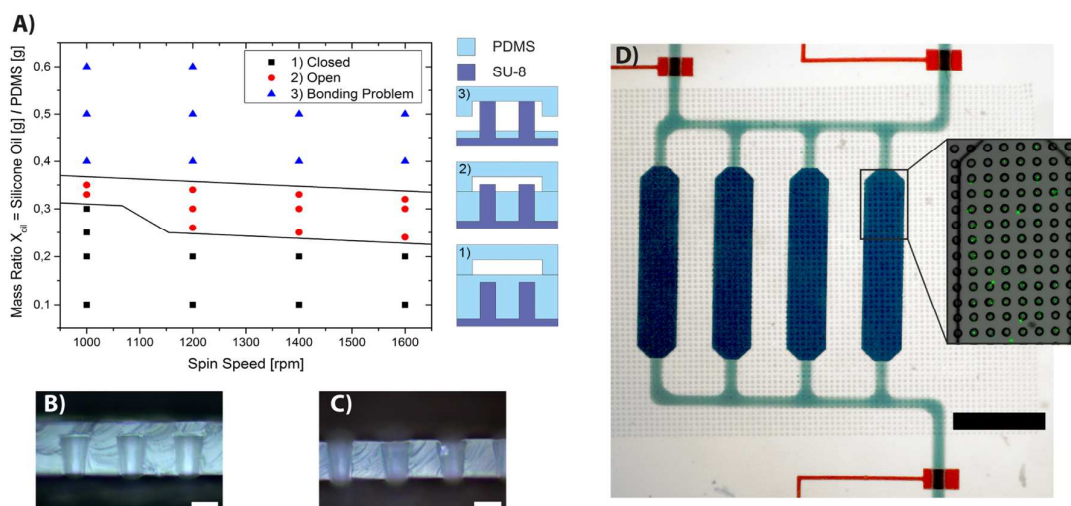
20 To achieve this, we designed an mLSI chip with a PM on a glass substrate forming
21 cavities as the retaining structure for the beads or cells. The chip layout is shown in
22 figure 3D where the bottom, middle, and top layer are the PM, flow and control layer,
23 respectively. The PM was prototyped from an array of SU-8 poles with a diameter,
24 height, and pitch distance of 20, 20, and 40 μm respectively; the total array size was
25 4 mm \times 4 mm. To achieve a PM thickness of $<20 \mu\text{m}$, we lowered the viscosity of the
26 PDMS with the silicone oil Element 14 PDMS 50-E. Due to its PDMS basis we
27 assumed that the components of the silicon oil are permanently cross-links within the
28 Pt catalyzed curing process to the base material of the PDMS. To test this we
29 performed a swelling experiment. For this PDMS blocks with a weight ratio of 6.5; 1;
30 2.5 of PDMS base material, curing agent, silicon oil respectively were swelled in
31 chloroform for 24 hours at RT. The samples were thereafter dried for 24 hours at
32 80 °C. The gel fraction, which is the weight after extraction and drying to the initial
33 weight of the DPMS blocks with the silicon oil was 85.1 ± 1.9 . Reference PDMS
34 blocks without the silicon oil had a gel fraction of $91 \pm 1.9\%$, which is in agreement
35 with previous reported gel fraction for off-ratio cured PDMS.²³ Thus we inferred that
36 the silicon oil indeed is cross-liked to the PDMS base unlike organic solvents.

1 The addition of Element 14 PDMS 50-E did not change the curing times of Sylgard
 2 184. We determined the optimal mass ratio between the silicone oil and PDMS, X_{Oil} ,
 3 and the corresponding spin speeds of the spin coating process, in order to achieve
 4 open through-holes within the thin PDMS membranes.

5 For each X_{Oil} , a chip was fabricated, and then horizontally cut to examine the state
 6 of the through-holes and to check whether they were open or closed. The result is
 7 shown in figure 3A. In the case of X_{Oil} , the ratios were between 0.25 and 0.35, and it
 8 was possible to obtain fully functional open through-holes demolded from a pole array.
 9 Below an X_{Oil} value of 0.25, the through-holes remained closed, whereas above a
 10 value of 0.35, the pole protrusion started hindering the process of layer bonding.
 11 Interestingly, increasing the spin speed from 1000 to 1600 rpm did not lead to a
 12 further thinning of the membrane, which indicates that the height of the PDMS
 13 membrane within this regime is predominantly set by the X_{Oil} ratio. For example we
 14 found that for a X_{Oil} ratio of 0.3 the PDMS membrane thickness was $12 \pm 3 \mu\text{m}$.

15 To demonstrate the function of PMs within the fully assembled mLSI chip, we
 16 captured fluorescently labeled beads with a diameter of $10 \mu\text{m}$. Beads with a
 17 concentration of $10^6/\text{mL}$ were flushed through the four microchambers of the mLSI
 18 platform with a flow rate of $1 \mu\text{L}/\text{min}$. Interrupting the flow allowed the beads to settle
 19 within the holes of the PM at the bottom of the chip. 82% of the holes were occupied
 20 with a bead after restarting and stopping the flow of the bead solution thrice for a
 21 period of 1 minute. The geometry of the pore array within the mLSI chip layout was
 22 not optimized for obtaining a high degree of bead occupancy. It is expected that in
 23 conjugation with the pillars and the other flow line barriers, higher degrees of cell or
 24 bead occupancies are achievable.

25



26

1 Figure 3. Fabrication of the perforated PDMS membranes with different mass ratios of
2 silicone oil from the C_4F_8 coated molds. **A)** The plot shows the spin speeds required
3 to obtain open through-holes within the PDMS layers, with different mass ratios of the
4 silicone oil. The wafer with the array of 20 μm high SU-8 pillars was coated with C_4F_8
5 before usage. Black, red, and blue dots denote the parameters at which the through-
6 holes in the cured PDMS were closed and opened, or when the chip could not be
7 assembled due to the steric hindrance of the protruding pillars. **B)** and **C)** Images of
8 the PDMS layer (16 and 12 μm in height) with closed and open through-holes. **D)**
9 Image of a three-layered PDMS chip with a perforated PDMS membrane on top of a
10 glass chip at the bottom forming cavities for retaining beads. The inset shows a
11 zoomed-in view of the perforated membrane at the bottom of a microchamber. The
12 holes/pores were filled with fluorescently labeled beads. The scale bars in figure B, C,
13 and D denote for 5, 5, and 750 μm , respectively.

14
15 In conclusion, we experimentally demonstrated the advantage of using a simple
16 super-hydrophobic coating procedure for PDMS molds. This technique could be used
17 to fabricate through-holes/via elements as well as perforated thin PDMS sheets at a
18 higher density for microfluidic large-scale integrated chip platforms. The C_4F_8 coatings
19 have been used previously for the production of high aspect ratio²⁴ for the coating of
20 PDMS, and for increasing the hydrophobicity of the material.²⁵ We show that reducing
21 the surface energy of the wafer and photoresist lead to robust release properties of
22 PDMS. In a parallel experiment, we found the same robustness upon reducing the
23 surface energy of the silicon molds, by coating the wafer with hydroxypropyl-methyl
24 cellulose.²⁶ The cellulose coating, however, is not stable over time and has to be
25 applied before each prototyping process. Therefore, it was not characterized in detail.
26 Moreover, for the pillar arrays with small pitch distances, the C_4F_8 coating could be
27 used to produce perforated PDMS membranes. Together with the silicone oil Element
28 14 PDMS 50-E, we introduced an alternative to organic solvents for lowering the
29 viscosity of PDMS and for fabricating thinner PDMS layers in the range of 10 – 40 μm .
30 Both the fabrication procedures can leverage large-scale integration microfluidics.
31 Future research in this area should focus on building more complex flow circuitries in
32 three dimensions.

34 **Acknowledgments**

35 This study was supported by the German Excellence Initiative of the German Federal and
36 State Governments (EXC-294 and GSC-4), and by the German Research Foundation
37 (Emmy-Noether Grant ME3823/1-1).

1

2 **References**

- 3 1. J. Melin and S. R. Quake, *Annu Rev Biophys Biomol Struct*, 2007, **36**, 213–231.
4 2. P. N. Duncan, T. V. Nguyen, and E. E. Hui, *Proc Natl Acad Sci USA*, 2013, **110**,
5 18104–18109.
6 3. N. S. G. K. Devaraju and M. A. Unger, *Lab Chip*, 2012, **12**, 4809.
7 4. J. McDonald and G. Whitesides, *Accounts Chem Res*, 2002, **35**, 491–499.
8 5. M. Meier, R. Sit, W. Pan, and S. R. Quake, *Anal Chem*, 2012, 121023083615005.
9 6. J. A. Weaver, J. Melin, D. Stark, S. R. Quake, and M. A. Horowitz, *Nature Physics*,
10 2010, **6**, 218–223.
11 7. E. P. Kartalov, C. Walker, C. R. Taylor, W. F. Anderson, and A. Scherer, *Proc Natl*
12 *Acad Sci USA*, 2006, **103**, 12280–12284.
13 8. J. Huft, D. J. Da Costa, D. Walker, and C. L. Hansen, *Lab Chip*, 2010, **10**, 2358.
14 9. N. Qu, X. Chen, H. Li, and D. Zhu, *Int J Adv Manuf Technol*, 2014, **72**, 487–494.
15 10. J. Choi, K.-H. Lee, and S. Yang, *J Micromech Microeng*, 2011, **21**, 097001.
16 11. A. L. Thangawng, R. S. Ruoff, M. A. Swartz, and M. R. Glucksberg, *Biomed*
17 *Microdevices*, 2007, **9**, 587–595.
18 12. W. Chen, R. H. W. Lam, and J. Fu, *Lab Chip*, 2011, **12**, 391–395.
19 13. C. F. Carlborg, T. Haraldsson, M. Cornaglia, G. Stemme, and W. van der Wijngaart, *J*
20 *Microelectromech S*, **19**, 1050–1057.
21 14. J. R. Rettig and A. Folch, *Anal Chem*, 2005, **77**, 5628–5634.
22 15. H. Wei, B.-H. Chueh, H. Wu, E. W. Hall, C.-W. Li, R. Schirhagl, J.-M. Lin, and R. N.
23 Zare, *Lab Chip*, 2011, **11**, 238.
24 16. Y. Wang, P. Shah, C. Phillips, C. E. Sims, and N. L. Allbritton, *Anal Bioanal Chem*,
25 2011, **402**, 1065–1072.
26 17. A. L. Thangawng, R. S. Ruoff, M. A. Swartz, and M. R. Glucksberg, *Biomed*
27 *Microdevices*, 2007, **9**, 587–595.
28 18. J. H. Koschwanez, R. H. Carlson, and D. R. Meldrum, *PLoS ONE*, 2009, **4**, e4572.
29 19. M. A. Unger, H. P. Chou, T. Thorsen, A. Scherer, and S. R. Quake, *Science*, 2000,
30 **288**, 113–116.
31 20. J. R. Anderson, D. T. Chiu, R. J. Jackman, O. Cherniavskaya, J. C. McDonald, H. Wu,
32 S. H. Whitesides, and G. M. Whitesides, *Anal Chem*, 2000, **72**, 3158–3164.
33 21. W. Y. Zhang, G. S. Ferguson, and S. Tatic-Lucic, *IEEE*, 2004, pp. 741–744.
34 22. C. Greiner, A. del Campo, and E. Arzt, *Langmuir*, 2007.
35 23. F. B. Madsen, I. Dimitrov, A. E. Daugaard, S. Hvilsted, and A. L. Skov, *Polym. Chem.*,
36 2013, **4**, 1700–1707.
37 24. L. P. Yeo, Y. H. Yan, Y. C. Lam, and M. B. Chan-Park, *Langmuir*, 2006, **22**, 10196–
38 10203.
39 25. A. D. Tserepi, M.-E. Vlachopoulou, and E. Gogolides, *Nanotechnology*, 2006, **17**,
40 3977–3983.
41 26. L. Gitlin, P. Schulze, and D. Belder, *Lab Chip*, 2009, **9**, 3000.
42